

Supporting Information

Photophysical and Photobiological Properties of Dinuclear Iridium(III) Bis-tridentate Complexes

Bingqing Liu,[†] Susan Monro,[‡] Levi Lystrom,[†] Colin G. Cameron,[§] Katsuya Colon,[§] Huimin Yin,[‡] Svetlana Kilina,[†] Sherri A. McFarland,^{*,‡,§} and Wenfang Sun^{*,†}

[†]*Department of Chemistry and Biochemistry, North Dakota State University, Fargo, ND 58108-6050, USA.*

[‡]*Department of Chemistry, Acadia University, 6 University Avenue, Wolfville, NS B4P 2R6, Canada.*

[§]*Department of Chemistry and Biochemistry, University of North Carolina at Greensboro, Greensboro, NC 27402-6170, USA.*

Experimental Details for Photobiological Activity Studies

Cellular Assays. *Ir(III) Complex Solutions.* Stock solutions of the chloride salts of the Ir(III) complexes were prepared at 5 mM in 10% DMSO in water and kept at -20°C prior to use. Working dilutions were made by diluting the stock solutions with pH 7.4 Dulbecco's phosphate buffered saline (DPBS). DPBS is a balanced salt solution of 1.47 mM potassium phosphate monobasic, 8.10 mM sodium phosphate dibasic, 2.68 mM potassium chloride, and 0.137 M sodium chloride (no Ca^{2+} or Mg^{2+}). DMSO in the assay wells was under 0.1% at the highest complex concentration.

Cell culture. *SK-MEL-28.* Adherent SK-MEL-28 malignant melanoma cells (ATCC HTB-72) were cultured in Eagle's Minimum Essential Medium (EMEM, Mediatech Media MT-10-009-CV) supplemented with 10% FBS and were incubated at 37°C under 5% CO_2 and passaged 2-3 times per week according to standard aseptic procedures. SK-MEL-28 cells were started at 200,000 cells/mL in 75 cm^2 tissue culture flasks and were subcultured when growth reached 550,000 cells/mL by removing old culture media and rinsing the cell layer once with Dulbecco's phosphate buffered saline (DPBS 1 \times , Mediatech, 21-031-CV), followed by dissociation of cell monolayer with 1 \times Trypsin-EDTA solution (0.25% (w/v) Trypsin/0.53 mM EDTA, ATCC 30-2101). Complete growth medium was added to the cell suspension to allow appropriate aliquots of cells to be transferred to new cell vessels. Complete media was prepared in 250 mL portions as needed by combining EMEM (225 mL) and FBS (25 mL, prealiquoted and heat inactivated) in a 250 mL Millipore vacuum stericup (0.22 μm) and filtering.

CCD-1064Sk. Adherent CCD-1064SK normal skin fibroblasts (ATCC CRL-2076) were cultured in Iscove's Modified Dulbecco's Medium (IMDM) supplemented with 10% FBS (PAA Laboratories, A15-701), were incubated at 37°C under 5% CO_2 and were passaged 2–3 times per week according to standard aseptic procedures. CCD-1064SK cells were started at 200,000 cells/mL in 75 cm^2 tissue culture flasks and were subcultured when growth reached approximately 550,000 cells/mL by removing old culture medium and rinsing the cell monolayer once with Dulbecco's phosphate buffered saline (DPBS 1 \times , Mediatech, 21-031-CV), followed by dissociation of the cell monolayer with trypsin-EDTA solution

(0.25% w/v Trypsin/0.53 mM EDTA, ATCC 30-2101). Complete growth medium was added to the cell suspension to allow appropriate aliquots of cells to be transferred to new cell vessels. Complete growth medium was prepared in 250 mL portions as needed by combining IMDM (225 mL) and FBS (25 mL, prealiquoted and heat inactivated) in a 250 mL Millipore vacuum stericup (0.22 μm) and filtering.

Cytotoxicity and photocytotoxicity

Cell viability experiments were performed in triplicate in 96-well ultra-low attachment flat bottom microtiter plates (Corning Costar, Acton, MA), where outer wells along the periphery contained 200 μL of DPBS (2.68 mM potassium chloride, 1.47 mM potassium phosphate monobasic, 0.137 M sodium chloride, and 8.10 mM sodium phosphate dibasic) to minimize evaporation from sample wells. Cells growing in log phase (SK-MEL-28 cells: ~550,000 cells/mL and CCD-1064Sk cells: ~500,000 cells/mL) with at least 93% viability were transferred in 50 μL aliquots to inner wells containing warm culture medium (25 μL) and placed in a 37 °C, 5% CO₂ water-jacketed incubator (Thermo Electron Corp., FormaSeries II, Model 3110, HEPA Class 100) for 3 h to equilibrate (and allow for efficient cell attachment in the case of both the SK-MEL-28 and CCD-1064Sk adherent cells). The Ir(III) complexes were serially diluted with DPBS and prewarmed at 37 °C before 25 μL aliquots of the appropriate dilutions were added to cells. PS-treated microplates were incubated at 37 °C under 5% CO₂ for 16 h drug-to-light intervals. Control microplates not receiving a light treatment were kept in the dark in an incubator, and light-treated microplates were irradiated under one of the following conditions: visible light (400–700 nm, 44 mW/cm²) using a 190 W BenQ MS 510 overhead projector or red light (625 nm, 52.5 mW/cm²) from an LED array (PhotoDynamic Inc., Halifax, NS). Irradiation times using these two light sources were approximately 38 and 32 min, respectively, to yield total light doses of 100 J/cm². Both untreated and light-treated microplates were incubated for another 48 h before 10 μL aliquots of prewarmed, sterile filtered 0.6 mM resazurin reagent (Sigma Aldrich Canada), according to a standard protocol, were added to all sample wells and subsequently incubated for another 3 h. Cell viability was determined on the basis of the ability of the resazurin redox indicator to be metabolically converted to a fluorescent dye by only live cells. Fluorescence was

quantified with a Cytofluor 4000 fluorescence microplate reader with the excitation filter set at 530 ± 25 nm and emission filter set at 620 ± 40 nm. EC_{50} values for cytotoxicity (dark) and photocytotoxicity (light) were calculated from sigmoidal fits of the dose-response curves using Graph Pad Prism 6.0 according to eq. 1, where y_i and y_f are the initial and final fluorescence signal intensities. For cells growing in log phase and of the same passage number, EC_{50} values are generally reproducible to within $\pm 25\%$ in the submicromolar regime, $\pm 10\%$ below $10 \mu\text{M}$, and $\pm 5\%$ above $10 \mu\text{M}$. Phototherapeutic indices (PIs), a measure of the therapeutic window, were calculated from the ratio of dark to light EC_{50} values obtained from the dose-response curves.

$$y = y_i + \frac{y_i - y_f}{1 + 10^{(\log EC_{50} - x) \times (\text{Hill slope})}} \quad (1)$$

DNA photocleavage assays

DNA photocleavage experiments were performed according to a general plasmid DNA gel mobility shift assay with $30 \mu\text{L}$ total sample volumes in 0.5 mL microfuge tubes. Transformed pUC19 plasmid ($3 \mu\text{L}$, $>95\%$ form I) was added to $15 \mu\text{L}$ of 5 mM Tris-HCl buffer supplemented with 50 mM NaCl (pH 7.5). Serial dilutions of the Ir(III) complexes were prepared in ddH₂O and added in $7.5 \mu\text{L}$ aliquots to the appropriate tubes to yield final Ir(III) complex concentrations ranging from 0.5 to $100 \mu\text{M}$. Then, ddH₂O ($4.5 \mu\text{L}$) was added to bring the final assay volumes to $30 \mu\text{L}$. Control samples with no Ir(III) complex received $12 \mu\text{L}$ of water. Sample tubes were kept at $37 \text{ }^\circ\text{C}$ in the dark or irradiated. Light treatments employed visible light (14 J/cm^2) delivered from a Luzchem LZC-4X photoreactor over the course of 30 min . After treatment, all samples (dark and light) were quenched by the addition of $6 \mu\text{L}$ of gel loading buffer (0.025% bromophenol blue, 40% glycerol). Samples ($11.8 \mu\text{L}$) were loaded onto 1% agarose gels cast with $1\times$ TAE (40 mM Tris-acetate, 1 mM EDTA, pH 8.2) containing ethidium bromide ($0.75 \mu\text{g/mL}$) and electrophoresed for 30 min at 80 V/cm in $1\times$ TAE. The bands were visualized using the Gel Doc-It Imaging system (UVP) with Vision Works software and further processed with the GNU Image Manipulation Program (GIMP).

Confocal microscopy

Sterile glass-bottom Petri dishes (MatTek) were coated with 200 μ L poly-L-lysine (Ted Pella) in a laminar flow hood under standard aseptic conditions. After a 1 h incubation period at 37 $^{\circ}$ C, 5% CO₂ in a water-jacketed incubator (Thermo Electron Corp., Forma Series II, Model 3110, HEPA class 100), the dishes were washed three times with sterile Dulbecco's phosphate buffered saline (DPBS, Mediatech, 21-031-CV) containing 2.68 mM potassium chloride, 1.47 mM potassium phosphate monobasic, 0.137 M sodium chloride, and 8.10 mM sodium phosphate dibasic, pH 7.4, and were left to dry uncovered at room temperature for approximately 15 min. SK-MEL-28 malignant melanoma cells (ATCC HTB-72) were then transferred in aliquots of 1.5 mL (approximately 100,000 cells) to the poly-L-lysine coated glass bottom Petri dishes and were allowed to adhere for 2-3 h in a 37 $^{\circ}$ C, 5% CO₂ water-jacketed incubator. Ir(III) complex (1.5 mL of a 50 μ M solution in sterile PBS prewarmed to 37 $^{\circ}$ C) was added to sample dishes (destined to receive either a dark or light treatment), which were returned to the incubator for 15 min prior to further treatment. Control dishes that did not contain the Ir(III) complex were also prepared. Light-treated samples were irradiated with visible light for 19 min from a 190 W BenQ MS 510 overhead projector (400–700 nm, power density 44 mW/cm², total light dose 50 J/cm²). Dark samples were covered with foil and placed in a drawer for the same amount of time. Cells were then imaged at 15 min post-treatment using a Carl Zeiss LSM 510 laser scanning confocal microscope with a 60 \times oil objective lens. Excitation was delivered at 458/488 nm from an argon–krypton laser, and signals were acquired through a 475 nm long-pass filter. Pinhole diameters for all the treatments were between 400-500 μ m. The images were collected and analyzed using the Zeiss LSM Image Browser Version 4.2.0.121 software (Carl Zeiss Inc.).

Table S1. Comparing the vertical excitation computed by ω B97XD and experimental values, for most of the complexes the transition energy for the first transition is around 0.70 eV whereas **Ir2** has 0.39 eV blue-shift compared to experimental values.

	Exp. / nm	Theor. / nm	ΔE / eV
Ir1	337	427	0.78
Ir2	383	436	0.39
Ir3	324	396	0.70
Ir4	337	413	0.68
Ir5	394	516	0.74
Avg.			0.66 \pm 0.15

Table S2. Natural transition orbitals (NTOs) for high energy transitions of **Ir1 - Ir5**. For transitions with quasi-degenerate transition orbitals only one pair of transition densities are shown and are indicated by *.

	State	Hole	Elec.		State	Hole	Elec.
Ir1	S ₇ *			Ir4	S ₈ *		
	291 nm				302 nm		
	$f = 0.717$				$f = 0.650$		
	S ₂₇ *				S ₁₉		
	264 nm				281 nm		
$f = 1.256$			$f = 0.449$				
S ₃₅ *			S ₂₃ *				
249 nm			270 nm				
$f = 0.674$			$f = 0.620$				
Ir2	S ₇ *			S ₃₃ *			
	292 nm			255 nm			
	$f = 0.707$			$f = 1.139$			
	S ₂₄ *			S ₉ *			
	270 nm			328 nm			
$f = 0.723$			$f = 0.395$				
S ₂₉ *			S ₁₅				
264 nm			305 nm				
$f = 1.121$			$f = 1.775$				
S ₃₉ *			S ₃₈ *				
249 nm			260 nm				
$f = 0.547$			$f = 0.889$				
Ir3	S ₂₃			S ₅₃ *			
	275 nm			247 nm			
	$f = 0.494$			$f = 0.718$			
	S ₃₂ *						
	260 nm						
$f = 0.437$							
S ₃₅ *							
249 nm							
$f = 0.571$							

Table S3. Emission characteristics of complexes **Ir1** - **Ir5** in different solvents at room temperature.

	$\lambda_{em} / nm (\tau_{em} / \mu s); \Phi_{em}$		
	THF	CH ₂ Cl ₂	Toluene (with 5% CH ₂ Cl ₂)
Ir1	586 (4.27); 6.8%	590 (2.71); 25%	584 (0.064); 2.0%
Ir2	579 (1.56); 0.4%	584 (1.78); 0.6%	555 (0.065), 675 (0.045); 0.4%
Ir3	620 (1.64); 3.3%	614 (1.54); 3.7%	620 (0.053); 0.6%
Ir4	581 (37.4); 32%	583 (69.7); 55%	581 (0.035); 3.4%
Ir5	651 (1.28); 3.9%	623 (1.61); 5.2%	672 (0.99); 1.2%

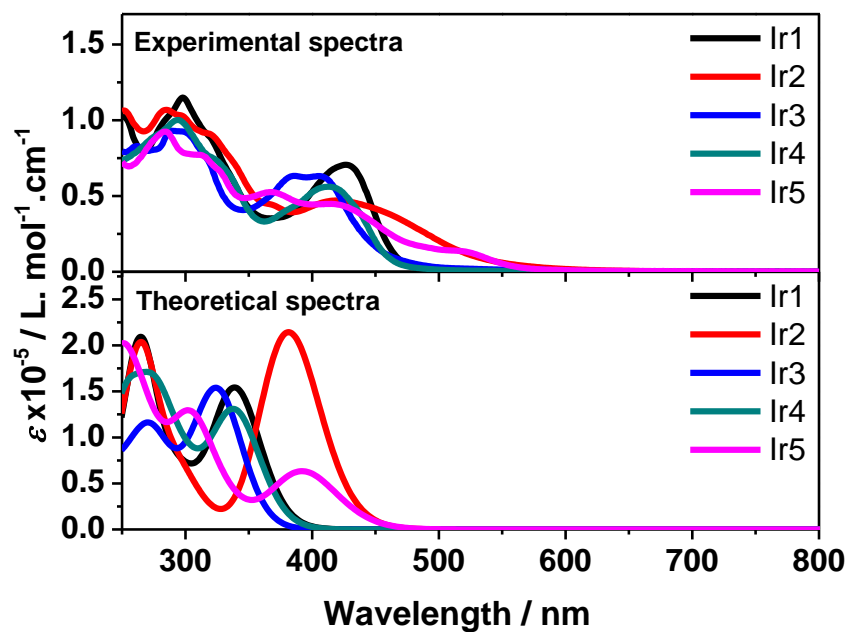


Figure S1. Comparison of the experimental UV-vis absorption spectra and the original calculated spectra with ω B97XD functional with linewidth of 0.2 eV in CH_3CN . The comparison shows that the shape of the theoretical spectra agrees but theoretically spectra are blue-shifted compared to experimental spectra.

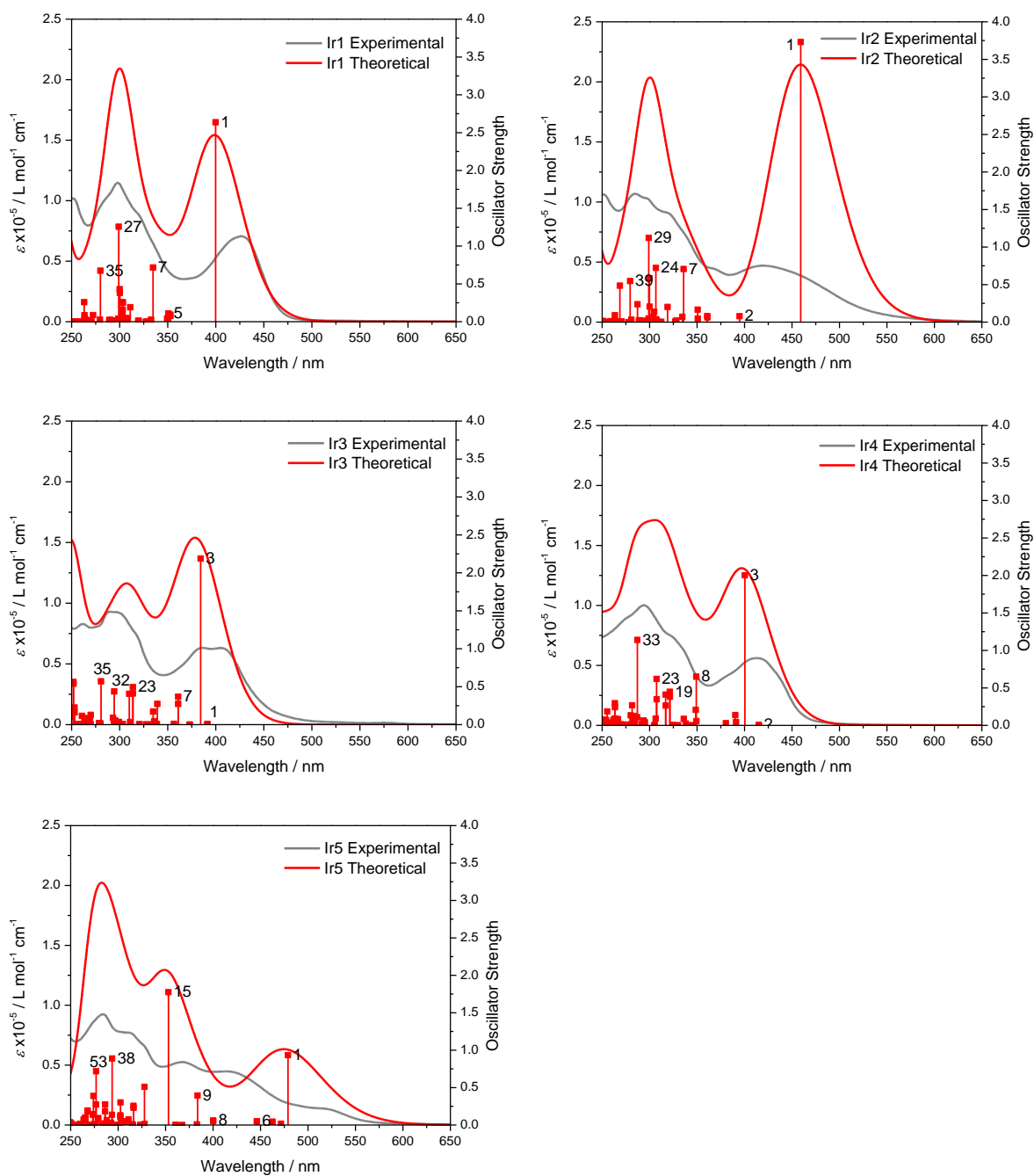


Figure S2. Comparison of the experimental and theoretical spectra for **Ir1 - Ir5** in CH_3CN . The theoretical spectra were computed using ωB97XD with mixed basis set. There was a redshift of 0.55 eV for the theoretical spectra.

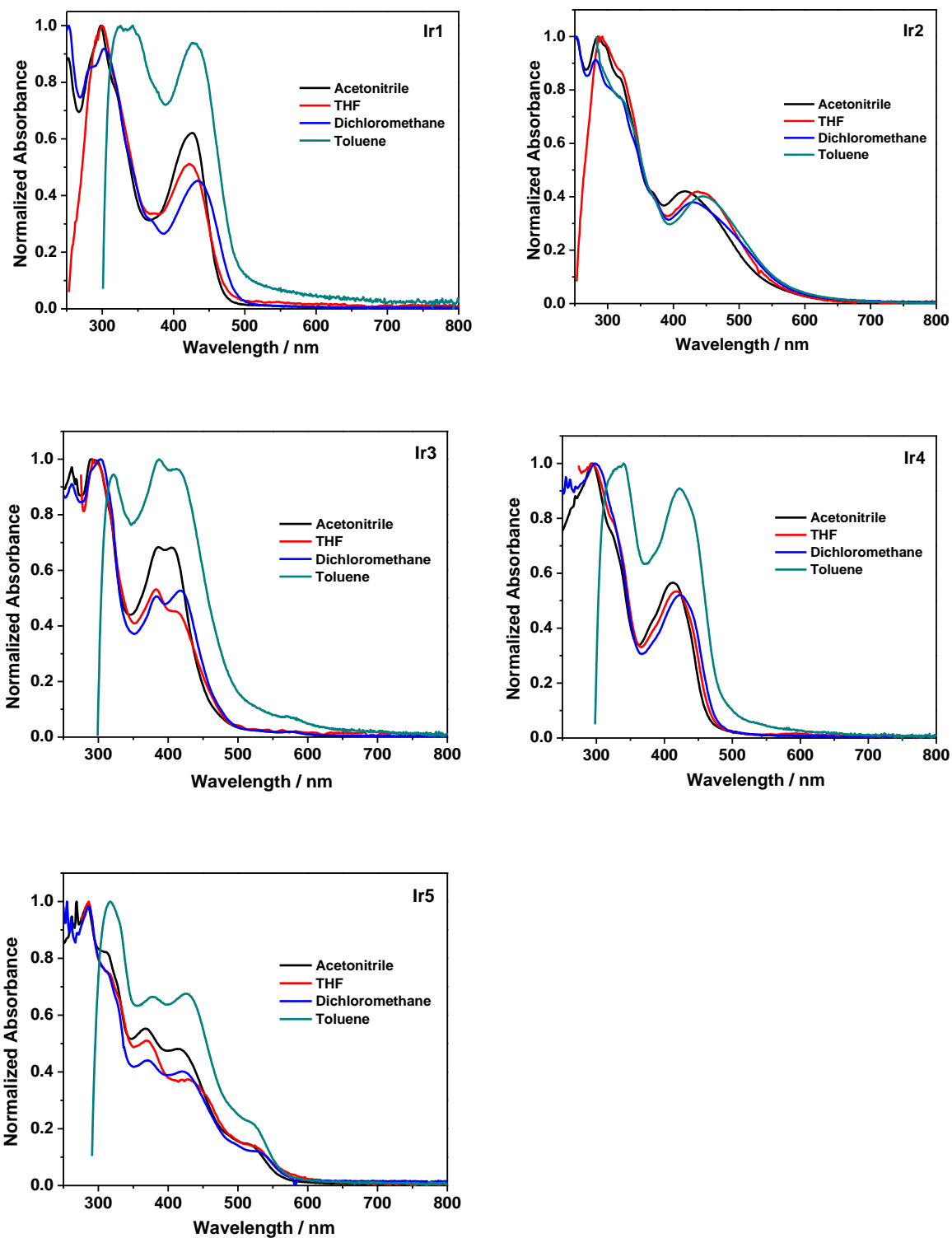


Figure S3. Normalized UV-vis absorption spectra of **Ir1** - **Ir5** in different solvents.

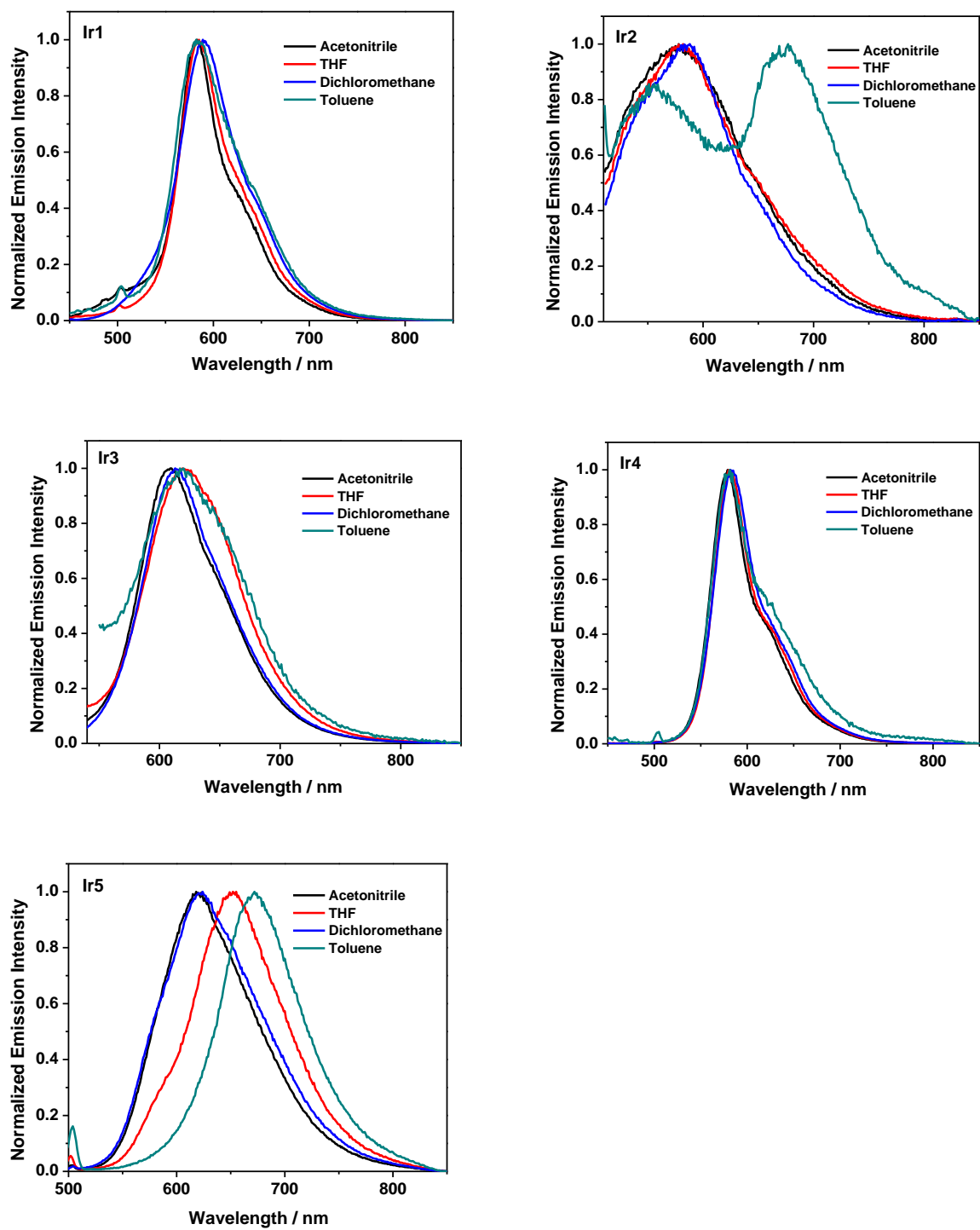


Figure S4. Normalized emission spectra of **Ir1** - **Ir5** in different solvents ($\lambda_{\text{ex}} = 436$ nm).

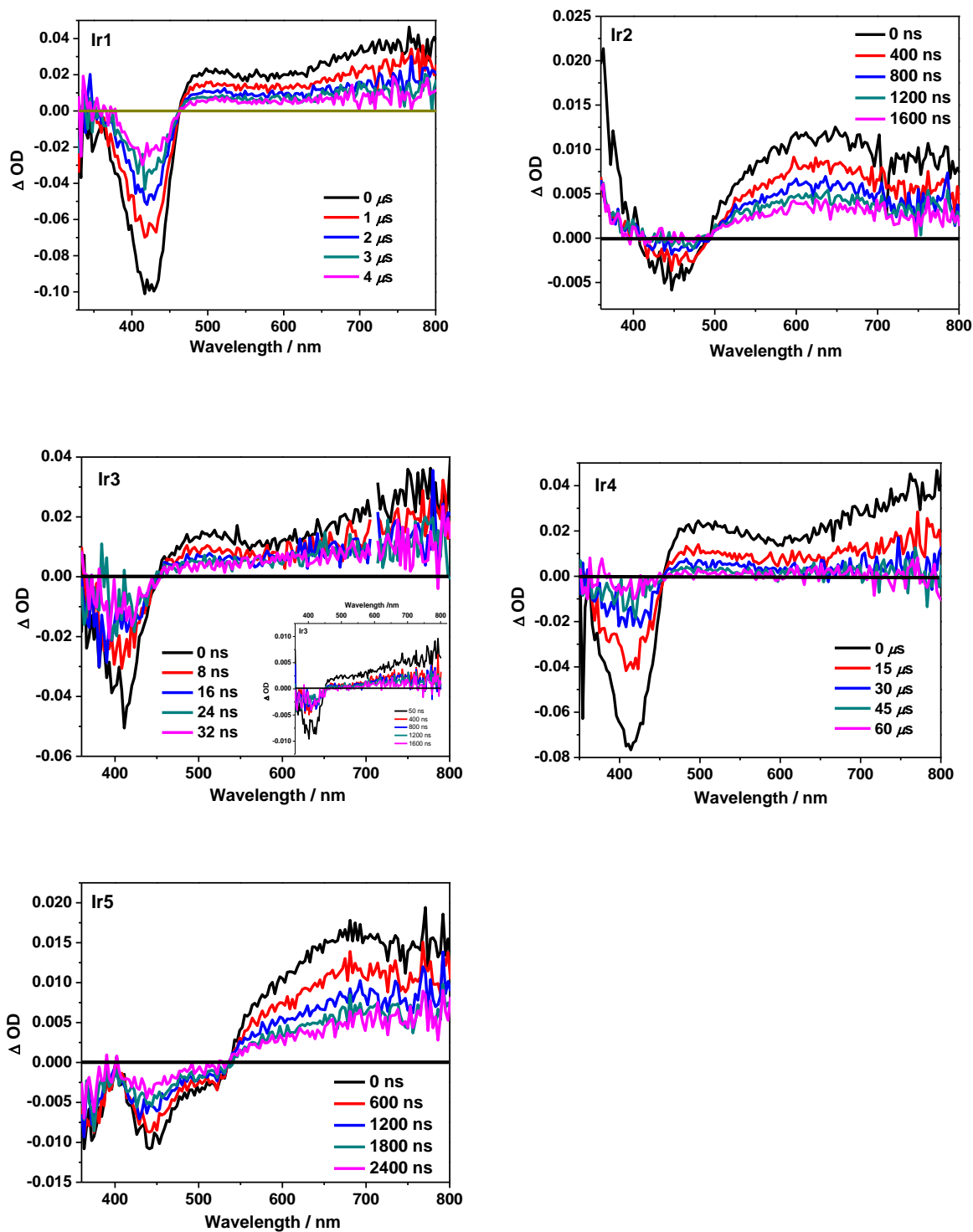


Figure S5. Nanosecond time-resolved transient differential absorption spectra of **Ir1 - Ir5** in acetonitrile. The inset in **Ir3** figure shows the time-resolved spectra at longer delay time. $\lambda_{\text{ex}} = 355 \text{ nm}$, $A_{355} = 0.4$ in a 1-cm cuvette.

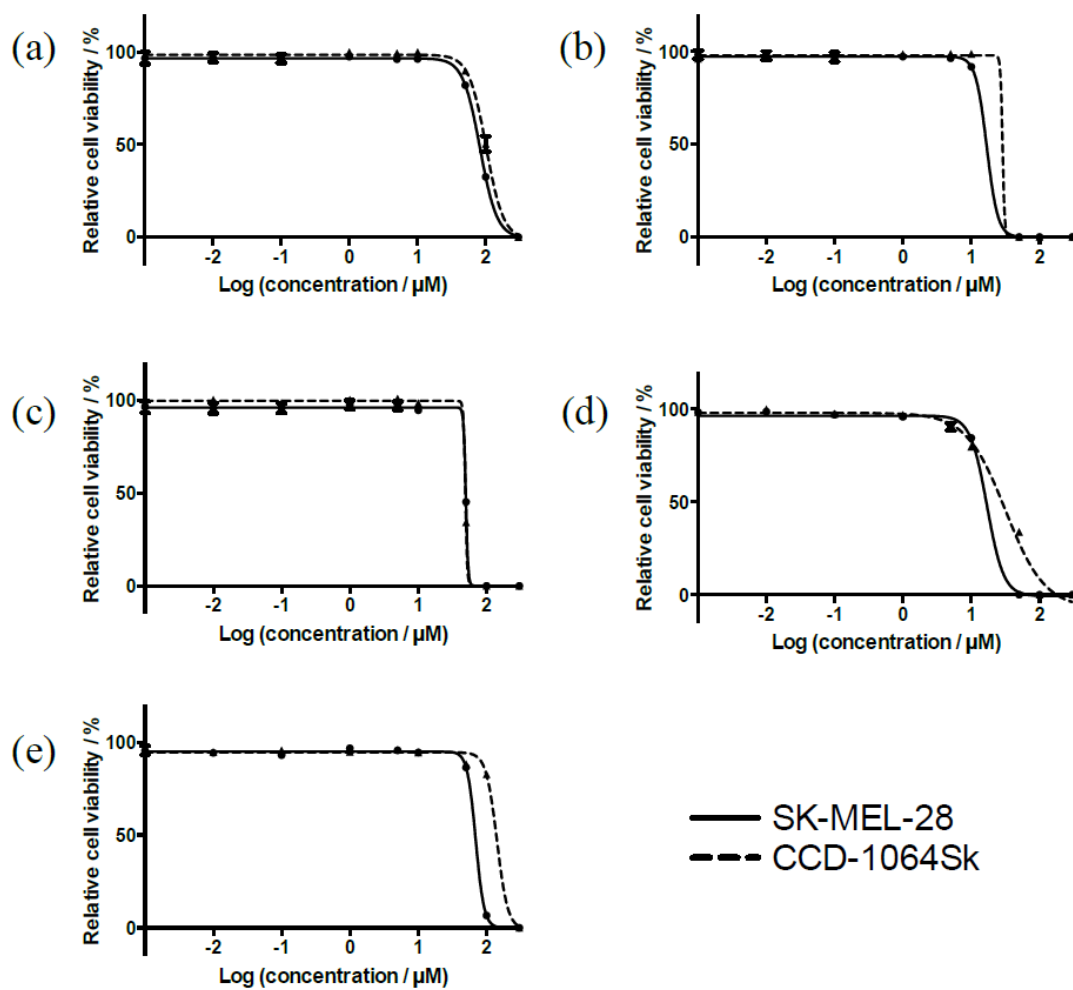


Figure S6. Comparison of cytotoxicity for complexes **Ir1** (a), **Ir2** (b), **Ir3** (c), **Ir4** (d) and **Ir5** (e) in SK-MEL-28 (solid line) and CCD-1064Sk cells (dotted line).

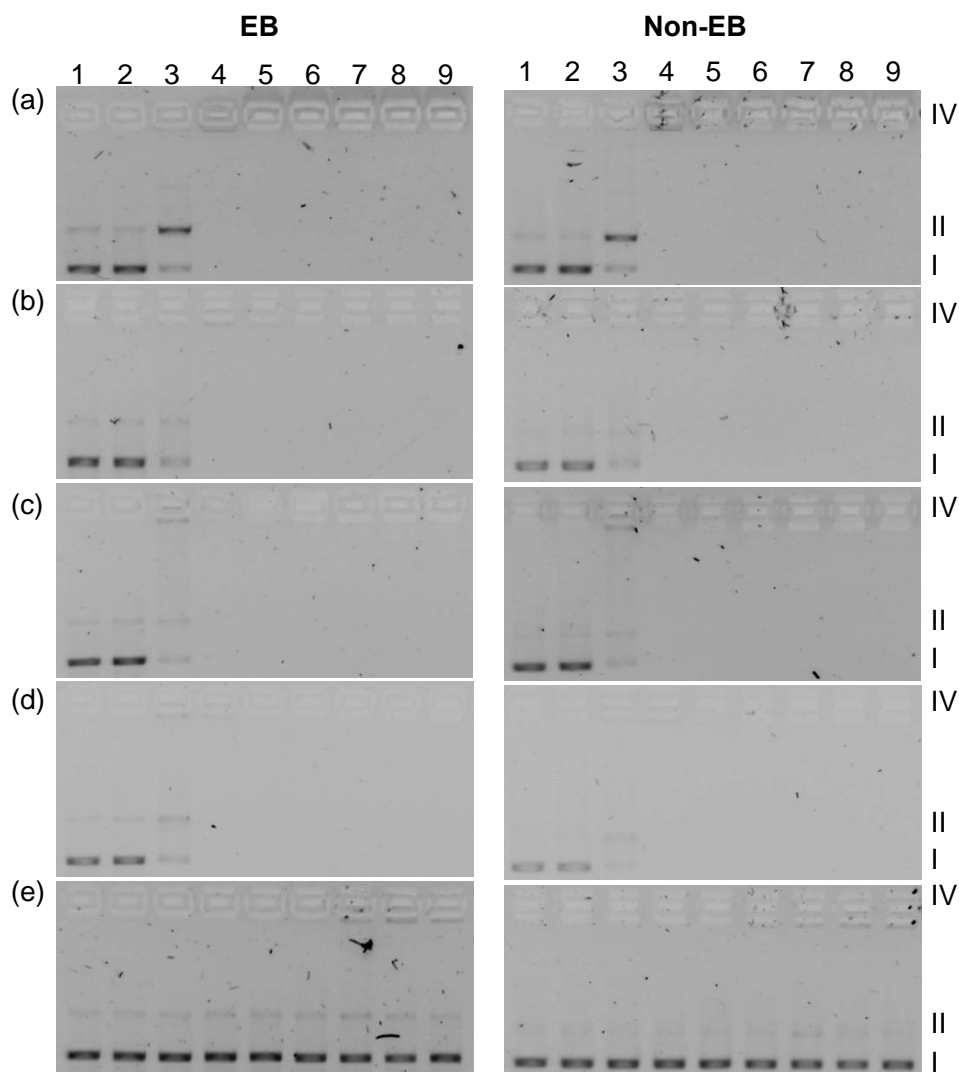


Figure S7. DNA photocleavage of pUC19 DNA (20 μM bases) dosed with metal complex (MC) **Ir1** (a), **Ir2** (b), **Ir3** (c), **Ir4** (d), **Ir5** (e) and visible light (14 J/cm^2). Gel mobility shift assays employed 1% agarose gels (0.75 $\mu\text{g}/\text{mL}$ ethidium bromide) electrophoresed in 1X TAE at 8 V/cm for 30 min. Lane 1, DNA only (-hv); lane 2, DNA only (+hv); lane 3, 5 μM MC (+hv); lane 4, 20 μM MC (+hv); lane 5, 40 μM MC (+hv); lane 6, 60 μM MC (+hv); lane 7, 80 μM MC (+hv); lane 8, 100 μM MC (+hv); lane 9, 100 μM MC (-hv). Forms I, II, and IV DNA refer to supercoiled plasmid, nicked circular plasmid, and aggregated plasmid, respectively.

REFERENCES (Note: These are the references provided in the manuscript but with full author list.)

(22) Stephenson, M.; Reichardt, C.; Pinto, M.; Wächtler, M.; Sainuddin, T.; Shi, G.; Yin, H.; Monro, S.; Sampson, E.; Dietzek, B.; McFarland, S. A. Ru(II) Dyads Derived from 2-(1-Pyrenyl)-1H-Imidazo[4,5-f][1,10]Phenanthroline: Versatile Photosensitizers for Photodynamic Applications. *J. Phys. Chem. A* **2014**, *118*, 10507–10521.

(24) Wang, L.; Yin, H.; Cui, P.; Hetu, M.; Wang, C.; Monro, S.; Schaller, R. D.; Cameron, C. G.; Liu, B.; Kilina, S.; McFarland, S. A.; Sun, W. Near-Infrared-Emitting Heteroleptic Cationic Iridium Complexes Derived from 2,3-Diphenylbenzo[g]Quinoxaline as in Vitro Theranostic Photodynamic Therapy Agents. *Dalton Trans.* **2017**, *46*, 8091–8103.

(61) Frisch, M. J.; Trucks, G. W.; Schlegel, H. B.; Scuseria, G. E.; Robb, M. A.; Cheeseman, J. R.; Scalmani, G.; Barone, V.; Mennucci, B.; Petersson, G. A.; Nakatsuji, H.; Caricato, M.; Li, X.; Hratchian, H. P.; Izmaylov, A. F.; Bloino, J.; Zheng, G.; Sonnenberg, J. L.; Hada, M.; Ehara, M.; Toyota, K.; Fukuda, R.; Hasegawa, J.; Ishida, M.; Nakajima, T.; Honda, Y.; Kitao, O.; Nakai, H.; Vreven, T.; Montgomery, J. J. A.; Peralta, J. E.; Ogliaro, F.; Bearpark, M.; Heyd, J. J.; Brothers, E.; Kudin, K. N.; Staroverov, V. N.; Keith, T.; Kobayashi, R.; Normand, J.; Raghavachari, K.; Rendell, A.; Burant, J. C.; Iyengar, S. S.; Tomasi, J.; Cossi, M.; Rega, N.; Millam, J. M.; Klene, M.; Knox, J. E.; Cross, J. B.; Bakken, V.; Adamo, C.; Jaramillo, J.; Gomperts, R.; Stratmann, R. E.; Yazyev, O.; Austin, A. J.; Cammi, R.; Pomelli, C.; Ochterski, J. W.; Martin, R. L.; Morokuma, K.; Zakrzewski, V. G.; Voth, G. A.; Salvador, P.; Dannenberg, J. J.; Dapprich, S.; Daniels, A. D.; Farkas, O.; Foresman, J. B.; Ortiz, J. V.; Cioslowski, J.; Fox, D. J. Gaussian 09, Revision D.01, *Gaussian, Inc.*,

Wallingford, CT, **2013.**